

# Direct extraction of hadronic form factors from elastic-scattering data

E. Martynov<sup>a\*</sup>, J.R. Cudell<sup>b†</sup>, A. Lengyel<sup>c‡</sup>

<sup>a</sup>Bogolyubov Institute for Theoretical Physics, Metrologicheskaja 14b, UA-03143, Kiev, Ukraine

<sup>b</sup>Institut de Physique, Université de Liège, 4000 Liège, Belgium,

<sup>c</sup>Institute of Electron Physics, Universitetska 21, UA-88000 Uzhgorod, Ukraine,

Non-forward elastic hadron-scattering data are collected and analysed within the Regge approach. Through an analysis of the data in small bins in  $t$ , we have directly extracted the pomeron trajectory and the hadronic form factors (or reggeon couplings). We found higher values than usually used for the intercept and for the slope of the soft pomeron trajectory. The presence of zeros in  $t$  for the effective hadronic form factors is emphasised.

## 1. Pomeron and reggeons at $t = 0$

A considerable effort [1] has recently been devoted to the reproduction of soft data at  $t = 0$  through analytical fits based on  $S$ -matrix theory. Three main forms for the pomeron,  $\ln \frac{s}{s_d}$ ,  $\ln^2 \frac{s}{s_t} + C$ , and simple poles  $\left(\frac{s}{s_1}\right)^\alpha$ , work reasonably well in the description of total cross sections at high energy ( $\sqrt{s} > 10$  GeV), however the simple-pole description fails if the energy threshold is lowered to  $\sqrt{s} > 5$  GeV, or if the real part of the amplitude is included, whereas the logarithmic forms achieve a good fit quality down to 5 GeV.

As shown in [2], if a “new” singularity with higher intercept  $\alpha_P(0) \approx 1.45$  (unitarized at  $\sqrt{s} > 100$  GeV) is added to the soft simple-pole-pomeron contribution, all three forms describe the data almost equivalently. On the other hand, the dispersion relations, with low-energy corrections for the real part of amplitudes, lead also to improved and comparable descriptions of the data at  $t = 0$  within these three pomeron models [3]. Thus, one cannot conclude which kind of pomeron best agrees with experiment on the sole basis of the available data on the total cross-sections,  $\sigma_t(s)$  and  $\rho(s) = \Re A(s, 0)/\Im A(s, 0)$ .

However, it is a very important task to cut down the list of pomeron models as this is needed to give unambiguous predictions for high energies. We believe that, in order to make progress in this direction, we have to extend the dataset, considering also the data for non-forward elastic hadron scattering.

## 2. Dataset for elastic scattering at $t \neq 0$

For total cross sections and real parts of amplitudes at  $t = 0$ , we have now a standard and commonly accepted set of experimental points [4]. Unfortunately, such a standard dataset for differential cross sections at  $t \neq 0$  is not established yet. However, the existing data are gathered in their original form, for example in the Durham Database [5].

We have collected, checked, and uniquely formatted about 10000 experimental points on differential cross sections for  $pp, \bar{p}p, \pi^\pm p, K^\pm p$  elastic scattering in the energy region  $\sqrt{s} > 4$  GeV and at all measured transferred momenta. The quality of the data obtained in various experiments varies quite strongly. For many sets, systematic errors are not given and for some others it is not clear from the original papers whether the systematic errors are included or not to the errors given in tables. Besides, it is well known that the normalisations of different sets are not in agreement, and are even sometimes in direct

\*e-mail: martynov@bitp.kiev.ua

†e-mail: JR.Cudell@ulg.ac.be

‡e-mail: sasha@len.uzhgorod.ua

contradiction.

Taking into account these circumstances, we have excluded a few subsets (11) out of a total of 200. These 11 subsets contradict even by eye the majority of the other subsets. We do not give here the detailed description of the data and individual references for the sets: this will be done in our forthcoming full paper [6].

### 3. Analysis of the data

A general goal of the analysis of the non-forward elastic-scattering data is to compare various pomeron models on the basis of a standard dataset, which should be as complete as possible. To simplify the analysis at the first stage, we restrict ourselves to the small- $|t|$  region, where the differential cross sections have a smooth behaviour (dominated by single pomeron and reggeon exchange terms). We analyse the data for elastic  $pp, \bar{p}p, \pi^\pm p$  and  $K^\pm p$  differential cross sections in the intervals

$$\begin{aligned} \sqrt{s} &> 5 \text{ GeV} \quad \text{for } pp \text{ and } \bar{p}p, \\ \sqrt{s} &> 6 \text{ GeV} \quad \text{for } \pi p \text{ and } Kp, \end{aligned} \quad (1)$$

$$|t|_{\min} = 0.05 \text{ GeV}^2 < |t| < |t|_{\max} = 0.85 \text{ GeV}^2$$

(There are some inconsistencies of the  $\pi p$  and  $Kp$  data at  $5 \text{ GeV} < \sqrt{s} < 6 \text{ GeV}$ , hence the exclusion of this region). To analyse the data, we considered a simplified parametrisation for the amplitudes, and then used it in the so-called method of overlapping bins.

**Amplitudes:** they were written in the form

$$A_{ab}^{\bar{a}b}(s, t) = P_{ab}(s, t) + R_{ab}^+(s, t) \pm R_{ab}^-(s, t), \quad (2)$$

where the pomeron term  $P_{ab}$ , the crossing-even term  $R_{ab}^+$  and the crossing-odd term  $R_{ab}^-$  are

$$P_{ab}(s, t) = \frac{g_{ab}(-is_{ab}/s_0)^{\alpha_P}}{-\sin(\pi\alpha_P/2)}, \quad (3)$$

$$R_{ab}^+(s, t) = \frac{g_{ab}^+(-is_{ab}/s_0)^{\alpha_+}}{-\sin(\pi\alpha_+/2)}, \quad (4)$$

$$R_{ab}^-(s, t) = \frac{ig_{ab}^-(-is_{ab}/s_0)^{\alpha_-}}{\cos(\pi\alpha_-/2)}, \quad (5)$$

with  $s_0 = 1 \text{ GeV}^2$  and  $s_{ab} = s - m_a^2 - m_b^2 + t/2 \propto f(t) \cos \theta_t$ ,  $\cos \theta_t$  being the scattering angle in

the  $t$ -channel. We consider the crossing-even and crossing-odd reggeons as effectively describing exchange-degenerate  $f - a_2$  and  $\omega - \rho$  contributions. The couplings  $g$  and trajectories  $\alpha$  are the constants determined from the fit in each  $t$ -bin.

**Overlapping bins:** Let us define the elementary bin:  $\tau < -t < \tau + \Delta t$ . If the  $s$ -dependence of the above amplitudes is roughly correct, we can determine the values of the trajectories and couplings in a given bin, provided  $\Delta t$  is small enough. Performing such fit for  $\tau = |t|_{\min} + k \cdot \delta t$ ,  $k = 1, 2, \dots, k_{\max}$ , we scan all data from  $|t|_{\min}$  up to  $|t|_{\max}$  and extract an effective  $t$ -dependence of trajectories and form factors or couplings. A few remarks regarding the method are to be noted:

1. The length of the bin should be not too big because of the simplified parametrisation and not too small in order to contain a reasonable number of points for each process. We take  $\Delta t = 0.025 \text{ GeV}^2$ .
2. We have chosen  $N_{\min} = 4$  as the minimal number of points for each process, thus taking into account only bins with 24 points or more.
3. We take for the shift from bin to bin  $\delta t = 0.01 \text{ GeV}^2$ . Wide variations of  $\Delta t$  and  $\delta t$  do not change the conclusions.
4. The fact that  $d\sigma/dt$  decreases almost exponentially with  $|t|$  is important even for small  $\Delta t$ . In each bin, we have written all couplings in the form  $g \rightarrow g(t) = g \exp(b(t - \tau))$ . The constants  $g$  (effective couplings at the first point ( $t = \tau$ ) of the corresponding bin) are discussed below.

**Reggeon (“ $f$ ” and “ $\omega$ ”) trajectories:** we are faced with the problem of the crossing-even and crossing-odd reggeon terms. Let us to call them as “ $f$ ” and “ $\omega$ ” contributions. They are badly determined from the fit. The obtained values of trajectories,  $\alpha_+$  and  $\alpha_-$ , as well as  $g^\pm$ , if left free, have a big dispersion from bin to bin. This is caused mainly by the inconsistencies in nor-

malisation of the many subsets. To restrict this randomness, we used the intercepts and slopes of  $f$  and  $\omega$  trajectories from the fits at  $t = 0$  and from the spectroscopic data [1,3,4,7]. Namely, we fixed the  $\omega$  trajectory using  $\alpha_- = 0.445 + 0.908 t$ . For the  $f$  trajectory we considered two variants, “maximal”  $\alpha_+ = 0.697 + 0.801 t$  and “minimal”  $\alpha_+ = 0.615 + 0.820 t$ .

#### 4. The results

The results obtained in the bin-analysis of the differential cross sections are shown in Figs 1-5. The black (resp. grey) symbols in Figs. 1, 2 correspond to the maximal (resp. minimal)  $f$  trajectory.

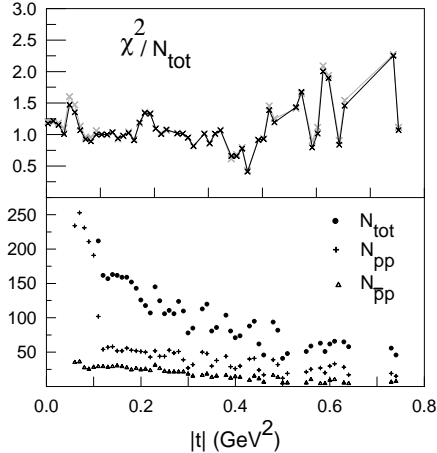


Figure 1.  $\chi^2$  per point and number of points (for  $pp$  and  $\bar{p}p$ ) for each bin.

A good description of the data ( $\chi^2/N_{tot} \approx 1$ , see Fig. 2) is achieved in the interval  $0.1 \text{ GeV}^2 \leq |t| \leq 0.5 \text{ GeV}^2$ . We can thus treat this interval as the first diffraction cone.

**Pomeron trajectory:** one can see from Fig. 2 that data do not confirm the “standard” values of the soft pomeron trajectory [8]. We indeed obtain

$$\alpha_P(0) = 1.084 - 1.096 \quad (6)$$

$$\alpha'_P = 0.3 - 0.33 \text{ GeV}^{-2} \quad (7)$$

instead of  $\alpha_P(0) = 1.0808$  and  $\alpha'_P = 0.25 \text{ GeV}^{-2}$ .

**Pomeron couplings** Fig. 3 shows that, in the  $pp$  and  $\bar{p}$  case, the dependence of  $g_{ab}$  on  $t$  is not

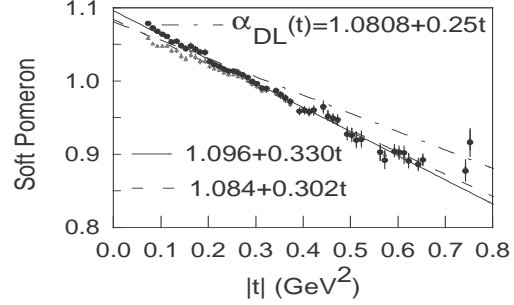


Figure 2. Fitted pomeron trajectory. The dashed-dotted line corresponds to the standard pomeron trajectory [8], and the two other lines to our fit to the extracted trajectory for minimal and maximal  $f$  trajectories.

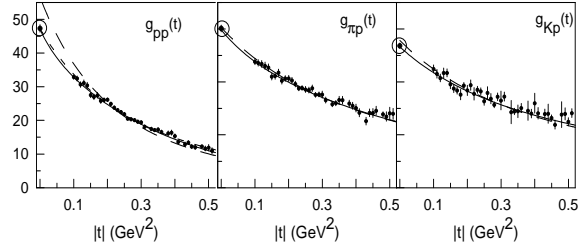


Figure 3. Pomeron couplings, points inside circles are added from the fit at  $t = 0$ . The long-dashed line corresponds to the parametrisation (8), the short-dashed line to a dipole form (9), and the solid line to the sum of two exponentials (10).

described perfectly ( $\chi^2/N_{dof} = 2.92$ ) by the expression

$$g_{ab}(t) = g_{ab} \left[ \frac{1 - t/1.269}{(1 - t/3.519)(1 - t/0.71)^2} \right]^2 \quad (8)$$

given in [8]. They are much better described ( $\chi^2/N_{dof} = 0.95$ ) by a simple dipole form

$$g_{ab} \left[ \frac{1}{(1 - t/3.519)(1 - t/0.661)} \right]^2 \quad (9)$$

or by the sum of two exponentials ( $\chi^2/N_{dof} = 0.92$ )

$$g_{ab} [0.08 \exp(12.69 t) + 0.92 \exp(1.27 t)]^2. \quad (10)$$

**Reggeon couplings:** the effective couplings of  $f$  and  $\omega$  reggeons both have at least one zero.

(Figs. 4 - 5). For the  $\omega$  contribution, this is a well-known feature, related to the crossover effect (differential cross sections of  $ab$  and  $\bar{a}b$  cross at small  $|t|$ ) discovered a long time ago in several experiments. However the zeros in the  $f$ -reggeon couplings are highly unexpected.

The detailed analysis of the results for the  $t$ -dependence of the effective couplings will be performed in a forthcoming full paper [6]. Here we give only some properties of the derived couplings in the case of the maximal  $f$  trajectory.

**Crossing-odd couplings:** Fig. 4 shows their extracted values and a fit to a single exponential multiplied by the factor  $1 + t/t_\omega$ . This leads to the following values for the zeros (in  $\text{GeV}^2$ ):

$$t_\omega = -0.12 (pp) \quad = -0.14 (\pi p) \quad = -0.15 (Kp)$$

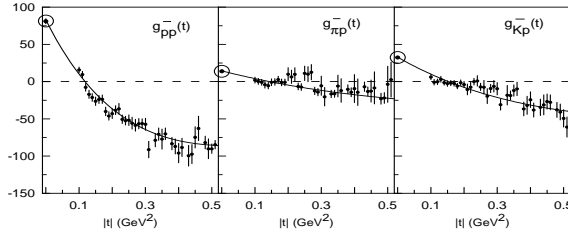


Figure 4.  $\omega$ -reggeon couplings, points inside circles are added from the fit at  $t = 0$ .

**Crossing-even reggeon couplings:** Fig. 5 shows that the same procedure as for the  $\omega$  couplings gives zeros of the  $f$  couplings at

$$t_f = -0.6 (pp) \quad = -0.33 (\pi p) \quad = -0.29 (Kp)$$

again in  $\text{GeV}^2$ .

As a conclusion to this short note, we would like to point out that the interpretation of the zeros in the form factors is not yet clear. Our attempts to perform a global fit of the various analytical models to the data failed when double re-scatterings (even with arbitrary strength) were included. Only the explicit account of zeros allows to describe well the full set of data in the first cone region, however it leads to low slopes for the  $f$  and  $\omega$  trajectories. A more thorough investigation of the problem is in progress.

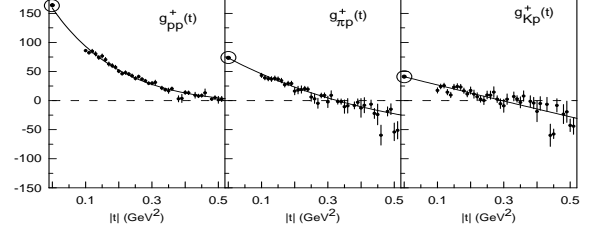


Figure 5.  $f$ -reggeon couplings, points inside circles are added from the fit at  $t = 0$ .

## REFERENCES

1. J.R. Cudell *et al.* [COMPETE Collaboration], Phys. Rev. D **65** (2002) 074024 [arXiv:hep-ph/0107219]; Phys. Rev. Lett. **89** (2002) 201801 [arXiv:hep-ph/0206172]; K. Hagiwara *et al.* [Particle Data Group Collaboration], Phys. Rev. D **66** (2002) 010001.
2. J.R. Cudell, E. Martynov, O. Selyugin, A. Lengyel, Phys. Lett. B **587** (2004) 78 [arXiv:hep-ph/0310198].
3. J.R. Cudell, E. Martynov, O. Selyugin, Ukr. J. Phys. **48** (2003) 1272, [arXiv:hep-ph/0307254].
4. <http://wwwppds.ihep.su:8001/hadron.html>.
5. <http://durpdg.dur.ac.uk/HEPDATA/>.
6. J.R. Cudell, E. Martynov, and A. Lengyel, in preparation.
7. P. Desgrolard, M. Giffon, E. Martynov and E. Predazzi, Eur. Phys. J. C **18**, 555 (2001) [arXiv:hep-ph/0006244].
8. A. Donnachie, H.G. Dosch, P.V. Landshoff, O. Nachtmann, Pomeron Physics and QCD, Cambridge University press, 2002.